Journal of Neonatal Surgery
ISSN(Online): 2226-0439
Vol. 14, Issue 31s (2025)
https://www.jneonatalsurg.com

OPEN ACCESS

Comparative Evaluation of Conventional and Advanced MRI Sequences in Detecting White Matter Abnormalities

Dheeraj Kumar[1*], Rajul Rastogi[2]

[1]MRIT, Ph.D. (Radio-Imaging) Pursuing Radiological Imaging Techniques, College of Paramedical Technology, Teerthanker Mahaveer University, Delhi Road, Moradabad, Uttar- Pradesh, INDIA. 244001

[1]School of Health Sciences, Chhatrapati Shahu Ji Maharaj University, Kanpur, Pradesh, INDIA. 208024

[2]Professor, MD Radio-Diagnosis at Teerthanker Mahaveer Medical College & Research Center Teerthanker Mahaveer University, Delhi Road, Moradabad, Uttar- Pradesh, INDIA. 244001

[*]**Corresponding Author:**

Dheeraj Kumar,

Email ID: dheeraj199494@gmail.com

Orchid Id: 0000-0003-4285-8104

Cite this paper as: Dheeraj Kumar, Rajul Rastogi, (2025) Comparative Evaluation of Conventional and Advanced MRI Sequences in Detecting White Matter Abnormalities. *Journal of Neonatal Surgery*, 14 (31s), 554-570.

ABSTRACT

Background: White matter (WM) abnormalities underlie a range of neurological diseases, such as multiple sclerosis, vascular dementia, and traumatic brain injury. Standard MRI sequences (T2-weighted, T2 FLAIR, DWI/ADC) are standardly employed for WM lesion detection but possibly insensitive to microstructural alterations. More sophisticated methods such as Diffusion Tensor Imaging (DTI) and Double Inversion Recovery (DIR) provide enhanced WM characterization but need systematic evaluation against standard approaches.

Aim: This research endeavoured to contrast the diagnostic accuracy of routine and high-end MRI sequences for the identification of WM abnormalities, determining lesion conspicuity, and evaluating microstructural integrity.

Materials and Methods: A cross-sectional study was conducted on 44 patients (mean age: 41.11 ± 13.51 years; 54.5% female) with suspected WM pathology. Conventional (T2W, T2 FLAIR, DWI/ADC) and advanced (DTI, DIR) sequences were performed on a 1.5T MRI scanner. Quantitative analysis included lesion size, fractional anisotropy (FA), mean diffusivity (MD), and qualitative assessment by radiologists. Statistical analyses (paired t-tests, Wilcoxon signed-rank, Chi-square, Spearman's correlation) were performed using SPSS ($p < 0.05$).

Results: Lesion distribution analysis demonstrated that the most frequently affected area was subcortical white matter, with involvement seen in 31.8% of the cases on T2-weighted (T2W) imaging and 34.1% on T2 fluid-attenuated inversion recovery (FLAIR) sequences. Among the cerebral lobes, the frontal lobe had the greatest lesion burden at 38.6%, followed by the occipital lobe at 34.1%. Regarding lesion conspicuity, no statistically significant difference existed between double inversion recovery (DIR) sequences and T2 FLAIR sequences ($p = 0.560$). Diffusion tensor imaging (DTI) values, i.e., fractional anisotropy (FA) with a mean of 0.43 ± 0.097 and mean diffusivity (MD) with a mean of 0.00080 ± 0.0001 mm^2/s, were not significantly different in patients with and without white matter tract abnormalities ($p > 0.05$). Temporal lobe lesions were all but chronic and were found to approach statistical significance ($p = 0.059$), with the likelihood ratio test demonstrating this relationship ($p = 0.015$).

Conclusion: Standard MRI sequences are still effective for WM lesion detection, and DTI and DIR offer additional microstructural and cortical lesion information. T2 FLAIR should be used for standard screening, with DTI and DIR confined to specialist use. High-field MRI and histopathological correlations should be investigated in further studies.

Keywords: *White matter abnormalities, MRI, Diffusion Tensor Imaging (DTI), Double Inversion Recovery (DIR), T2 FLAIR, lesion detection, neuroimaging.*

1. INTRODUCTION

White matter (WM) integrity is crucial for efficient and synchronized transmission of neural signals between brain areas. The white matter, comprising predominantly myelinated axonal tracts, facilitates interaction between cortical and subcortical areas and is critical to many cognitive and motor behaviors [1,6]. White matter pathological alterations are typical of numerous neurologic conditions, including multiple sclerosis (MS), leukodystrophies, vascular dementia, traumatic brain injury (TBI), and neurodegenerative disorders [2,5,11]. It is thus crucial for disease prognosis, monitoring, and treatment planning to detect white matter abnormalities early and reliably. Traditional magnetic resonance imaging (MRI) techniques, represented in Figure 1, such as T2-weighted (T2W), T2 fluid-attenuated inversion recovery (FLAIR), and diffusion-weighted imaging (DWI) with apparent diffusion coefficient (ADC) mapping, are employed on a daily basis in clinical neuroimaging for white matter lesion detection and characterization [3,6]. T2W and FLAIR sequences are very sensitive to demyelination and gliosis hyperintense signal changes, but DWI/ADC provides information on cytotoxic edema and cellular packing density useful in acute ischemia and infections is showing in Figure 1 [3,10].

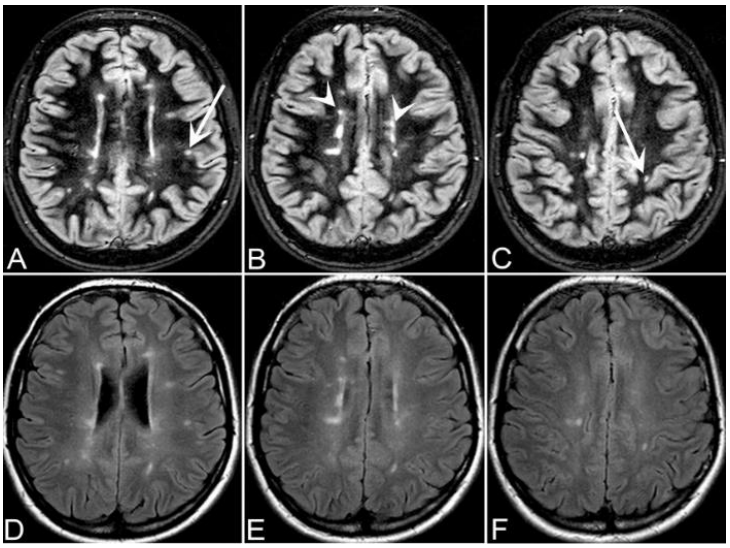

Figure 2 The set of axial FLAIR MRI scans (A–F) demonstrates differential degrees and patterns of white matter hyperintensities (WMHs) that are typically observed in clinical and research neuroimaging. Figure A-shows confluent periventricular and deep white matter hyperintensities prominently affecting the centrum semiovale, with a hyperintense lesion extending radially from the lateral ventricle towards the subcortical white matter features typical of chronic small vessel ischemia or demyelination. Image B-is characterized by periventricular caps and bands around the frontal horns and body of the lateral ventricles, which are consistent with periventricular ischemia or gliosis, and indicative of Fazekas grade 2 small vessel disease. Image C-demonstrates both periventricular and juxtacortical hyperintensities, discrete lesions near the cortical ribbon that make one suspect demyelinating diseases such as multiple sclerosis, particularly due to their orientation in a fashion similar to Dawson's fingers. Conversely, Image D-illustrates a normally appearing brain without WMHs, which is being used as a control image to bring out the lack of ischemic or demyelinating changes. Image E-illustrates mild deep white matter hyperintensities, particularly in the frontal lobes, as small punctate foci that can be indicative of early microvascular ischemic changes typically incidental in elderly patients. Lastly, Image F-depicts minimal or no WMHs detectable on imaging, with homogeneous white matter signal and no pathologic findings, most likely in a normal subject or with only very mild, nonspecific alterations. Together, the images demonstrate the range from normal white matter to moderate to severe pathology.

These sequences are typically non-specific and non-sensitive to find fine microstructural changes or to evaluate structural brain connectivity [4,5]. Advanced MRI sequences such as Diffusion Tensor Imaging (DTI) and Double Inversion Recovery (DIR) are more useful for the evaluation of white matter DTI, an advanced form of DWI, quantifies the direction of water molecule motion in axonal fibers and hence microstructural integrity with parameters such as fractional anisotropy (FA) and mean diffusivity (MD) Figure 3 [2,5,8]. DTI tractography can also visualize white matter tracts, providing information on derangement of connectivity in diseases [3,9]. DIR imaging, on the other hand, specifically suppresses signals from cerebrospinal fluid and white matter and emphasizes gray matter and white matter pathological alterations. This sequence is very effective in detecting cortical as well as juxtacortical lesions, which are often overlooked in routine imaging [13,14]. Current research has set the benefit of DTI and DIR for white matter abnormality detection in demyelinating disorders and early neurodegenerative alterations [4,12,13].

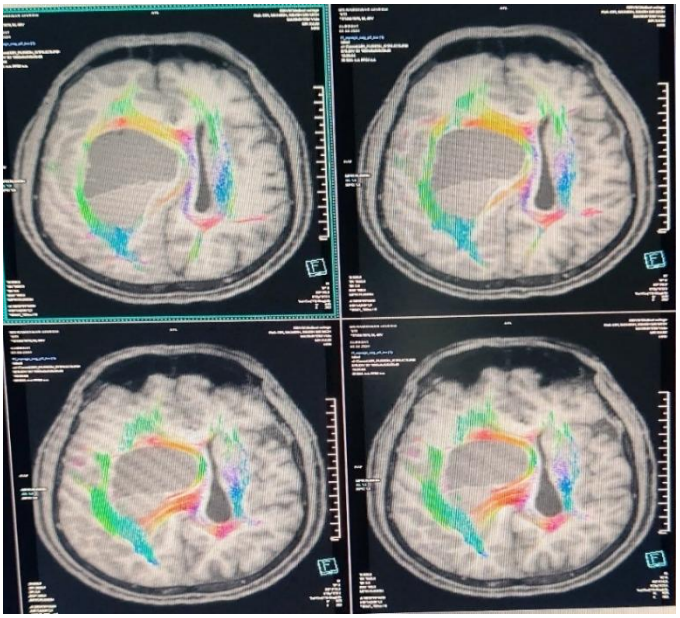

Figure 4 These MRI DTI tractography images provide a high-resolution, color-coded visualization of white matter fiber tracts in the brain. They are likely used in the context of neurological assessment, pre-surgical planning, or research into brain connectivity. The colored fibers indicate orientation-specific pathways critical for motor, cognitive, and sensory functions.

DIR increases lesion contrast, particularly in cortical regions, while DTI provides quantitative data indicative of axonal injury and demyelination [2,5,13]. While each has benefit separately, a systematic comparison between these new sequences and conventional imaging modalities in a clinical cohort is scarce. With increasing clinical reliance on MRI for neurological evaluation, there exists an urgent need to delineate the diagnostic advantages and ancillary roles of conventional and cutting-edge sequences in the diagnosis of white matter abnormalities. This study aims to compare methodically the standard MRI sequences (T2W, T2 FLAIR, DWI/ADC) with the cutting-edge sequences (DTI and DIR) to diagnose and characterize white matter lesions. In addition, the study seeks to quantify white matter tract integrity with DTI and lesion visibility in DIR at sites of white matter of anatomical significance. Through the clarification of the relative strengths and limitations of each imaging method, this research may be able to provide enhanced neuroimaging protocols, improved lesion detection, and improved clinical decision-making in white matter disease conditions.

2. METHODOLOGY

This cross-sectional observational hospital-based study was designed for comparing the diagnostic performance of reference and advanced magnetic resonance imaging (MRI) sequences in detecting white matter changes with special reference to measurement of white matter tract integrity. The study will be conducted in the Department of Radiodiagnosis of a tertiary care facility with a 1.5 Tesla SIEMENS MAGNETOM Avanto MRI machine. 44 patients between the age group 18-65 years with clinical suspicion of white matter pathology i.e., demyelinating conditions, ischemia, or post-inflammatory changes will be recruited on being provided written informed consent. Inclusion criteria require that the patients must be clinically indicated for MRI with suspected involvement of white matter and agree to receive conventional and high-tech sequences. Exclusion factors are MRI contraindications (e.g., metal implants, pacemaker), uncontrolled claustrophobia, intracranial surgery or trauma less than three months ago, and poor image quality. Standardized brain imaging with standard sequences T2-weighted (sagittal and axial), T2 FLAIR (axial), and DWI/ADC maps and advanced sequences like Diffusion Tensor Imaging (DTI) with a 32-direction protocol and Double Inversion Recovery (DIR) sequences will be performed in all subjects. Specialized workstations and image analysis software such as FSL and 3D Slicer [9,13] will be used for post-processing. Quantitative measures will include lesion volume and load, DTI such as fractional anisotropy (FA), mean diffusivity (MD), and axial/radial diffusivity in regions of interest (e.g., corpus callosum, periventricular white matter) as well as DIR-based scores on visibility on a 0–3 scale. Qualitative analysis will involve two blinded reads by experienced radiologists in terms of lesion conspicuity, localization, and diagnostic confidence, with agreement achieved by consensus. Primary outcome will be comparative evaluation of detection rate, visibility, and lesion load between conventional and advanced sequences. Secondary outcomes will include white matter tracts integrity in terms of FA and MD values and periventricular and juxtacortical lesion detectability in terms of DIR [2,13,14]. Statistical tests shall be performed with SPSS software version 25.0, using descriptive statistics, paired t-tests or Wilcoxon signed-rank tests, intraclass correlation coefficients (ICC), and correlation analyses (Pearson or Spearman) as necessary, at a significance level of $p < 0.05$ [10]. Institutional Ethics Committee clearance shall be obtained, and all data shall be handled in strict confidence.

3. RESULT AND ANALYSIS

Descriptive statistics were calculated to describe categorical variables of interest in the study. The gender distribution among the 44 participants yielded a nearly balanced representation, with a mean of 1.55 (SD = 0.504), showing a slight preponderance of females. There was no missing data for gender, T2-weighted (T2W) lesion site, T2 fluid-attenuated inversion recovery (T2 FLAIR) lesion site, or lobe of brain involvement according to DWI/ADC sequences. The average for lobe involvement was 1.98 (SD = 0.976), indicating frontal and occipital lobes were most commonly involved. The use of a value range of 3 for the values of lobe involvement (coded as 1 = Frontal, 2 = Occipital, 3 = Temporal, 4 = Parietal) also indicates lesion distribution extended across more than one lobe. These results provide the foundation for comparative studies intended to determine lesion visibility and white matter tract integrity between imaging modalities.

Table 1 Frequency Distribution of Gender Among Study Participants (N = 44)

Gender					
		Frequency	**Percent**	**Valid Percent**	**Cumulative Percent**
Valid	Male	20	45.5	45.5	45.5
	Female	24	54.5	54.5	100.0
	Total	44	100.0	100.0	

The gender split among the 44 patients showing in Table 2 studied was favorably inclined towards females. Of the total samples, 24 were female (54.5%) and 20 were male (45.5%). Frequency counts and valid percentages were applied to this split, ensuring data completeness with no missing values. Cumulative percentage indicates that women formed the rest of the cohort when adjusting for men to a total of 100%. This balanced distribution provides an unbiased comparative analysis of imaging parameters between genders in the study.

Table 3 Frequency Distribution of Lesion Locations on T2-Weighted Imaging Among Study Participants (N = 44)

T2W Lesion Location					
		Frequency	**Percent**	**Valid Percent**	**Cumulative Percent**
Valid	Deep white matter	12	27.3	27.3	27.3
	Juxtacortical	9	20.5	20.5	47.7
	Periventricular	9	20.5	20.5	68.2
	Subcortical	14	31.8	31.8	100.0
	Total	44	100.0	100.0	

T2-weighted (T2W) imaging disclosed varied lesion sites in the white matter areas among the subjects are showing in Table 4. The subcortical white matter was the most frequently encountered lesion site with 14 patients (31.8%). Deep white matter lesions were encountered in 12 cases (27.3%), and juxtacortical and periventricular areas each had 9 lesions (20.5%). These values reflect the reasonably uniform distribution of white matter lesions among anatomical regions with a predominance in the subcortical region. The sum of the percentage attained 100%, which ensured that the data were complete and enabled valid comparative and correlative analyses in later stages of the study.

Table 5 Frequency Distribution of Lesion Locations on T2 FLAIR Imaging Among Study Participants (N = 44)

T2 FLAIR Lesion Location					
		Frequency	Percent	Valid Percent	Cumulative Percent
Valid	Deep white matter	14	31.8	31.8	31.8
	Juxtacortical	7	15.9	15.9	47.7
	Periventricular	8	18.2	18.2	65.9

	Subcortical	15	34.1	34.1	100.0
	Total	44	100.0	100.0	

T2 fluid-attenuated inversion recovery (T2 FLAIR) imaging revealed a broad anatomical distribution of white matter lesions within the study group showing in Table 6. Subcortical white matter lesions were the most common, occurring in 15 subjects (34.1%), followed by deep white matter lesions in 14 (31.8%). Periventricular lesions were detected in 8 subjects (18.2%), and juxtacortical involvement was the least common, occurring in 7 patients (15.9%). The combined percentage was 100%, and no information was missing, providing strong validity to the distribution. The results indicate a mild preference for subcortical and deep white matter areas in T2 FLAIR lesion detection, reaffirming its use in detecting varied white matter pathology.

Table 7 Frequency Distribution of Lesion Location by Lobe of Brain Based on DWI/ADC Imaging (N = 44)

Lesion location Lobe of Brain (Frontal=1, Occipital=2, Temporal=3, Parietal=4)					
		Frequency	**Percent**	**Valid Percent**	**Cumulative Percent**
Valid	1	17	38.6	38.6	38.6
	2	15	34.1	34.1	72.7
	3	8	18.2	18.2	90.9
	4	4	9.1	9.1	100.0
	Total	44	100.0	100.0	

Lesion location according to diffusion-weighted imaging (DWI) and apparent diffusion coefficient (ADC) maps demonstrated the frontal and occipital lobes to be predominantly affected in the study group is showing in Table 8. In 44 subjects, 17 (38.6%) had lesions in the frontal lobe, and 15 (34.1%) had lesions in the occipital lobe. Temporal lobe lesions were noted in 8 patients (18.2%), and 4 cases (9.1%) demonstrated parietal lobe lesions. The overall percentage was 100%, signifying no missing values and a well-completed dataset. The results highlight the common vulnerability of the frontal and occipital lobes to white matter abnormalities in this population, providing valuable insights into regional vulnerability analysis as well as advanced imaging correlation.

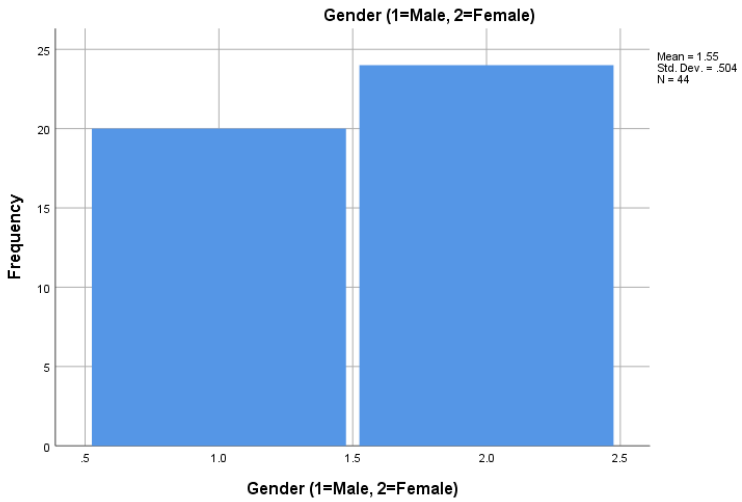

Figure 5 Frequency distribution of gender (1=Male, 2=Female) in a sample of 44 respondents, with a mean of 1.55 and standard deviation of 0.504.

The Figure 6 graph shows the distribution of gender in a dataset, where 1 is Male and 2 is Female. The mean of 1.55 indicates

a higher percentage of females in the sample, since the value is nearer to 2 (Female) than 1 (Male). The standard deviation of 0.504 implies moderate variation in the data. With the total sample size (N) being 44, the graph must represent the number or proportion of females and males, depicting the gender makeup of the surveyed population. The graphical form makes it easy to identify the gender skew, with females outnumbering the males in this specific dataset.

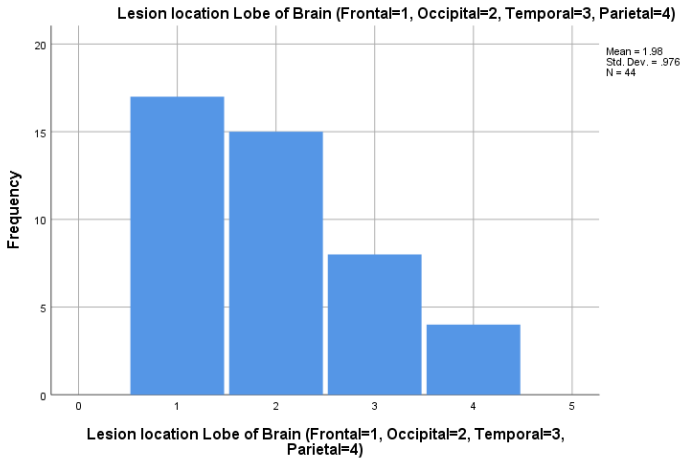

Figure 7 Frequency distribution of brain lesion locations (Frontal=1, Occipital=2, Temporal=3, Parietal=4) in a sample of 44 cases, with a mean of 1.98 and standard deviation of 0.976.

The Figure 8 chart displays the frequency distribution of brain lesion sites over four lobes: Frontal (1), Occipital (2), Temporal (3), and Parietal (4). The mean value of 1.98 indicates that the lesions tend to occur most frequently in the Occipital lobe or on either side of the border between the Frontal and Occipital lobes. The standard deviation of 0.976 points toward moderate variation in lesion sites. Since sample size (N) is 44, the chart most probably shows counts or proportions by each lobe and assists in determining trends in the prevalence of lesions. This visualization is useful in viewing the distribution of brain lesions and is essential in clinical or research applications.

Table 9 Descriptive Statistics for Continuous Variables Including Age, Lesion Size, and Diffusion Metrics (N = 44)

Descriptive Statistics					
	N	Minimum	Maximum	Mean	Std. Deviation
Age	44	19	64	41.11	13.508
T2W Lesion Size (mm)	44	3.20	14.700	9.16	3.360
FA Value	44	.200	.67	.43	.0971
MD Value	44	.0006	.0011	.00080	.0001
T2 FLAIR Lesion Size (mm)	44	4.0	17.00	9.943	3.503

Descriptive statistics were calculated for continuous variables such as patient age, T2W and T2 FLAIR lesion sizes, and diffusion tensor imaging (DTI) parameters Fractional Anisotropy (FA) and Mean Diffusivity (MD) is showing in Table 10. The ages of the participants varied from 19 to 64 years, with a mean age of 41.11 years (SD = 13.51), representing a wide adult population pertinent to white matter pathology. The average lesion size on T2W imaging was 9.16 mm (range: 3.2–14.7 mm), whereas lesions were slightly bigger on T2 FLAIR sequences, with an average measurement of 9.94 mm (range: 4.0–17.0 mm). These results describe fairly concordant lesion detection with both the conventional sequences, though with FLAIR providing a little more conspicuity. Diffusion measurements also differed among the study group. FA values were between 0.20 and 0.67 and had a mean of 0.43 (SD = 0.0971), whereas MD values were between 0.0006 and 0.0011 mm^2/s and had a mean of 0.00080 mm^2/s (SD = 0.0001). These diffusion measurements are indicative of the microstructural integrity of white matter tracts, with lower FA and increased MD generally indicating axonal damage or demyelination. The statistical stability and variation exhibited in this data form the basis for sound correlation and comparative studies that support the study's core and secondary aims.

Hypothesis Test Summary

	Null Hypothesis	Test	Sig.	Decision
1	The median of differences between Lesion Conspicuity Score (DIR) Likert scale and Lesion Conspicuity Score (T2 FLAIR) Likert Scale equals 0.	Related-Samples Wilcoxon Signed Rank Test	.560	Retain the null hypothesis.

Asymptotic significances are displayed. The significance level is .05.

Figure 9 Results of a Wilcoxon Signed Rank Test comparing Lesion Conspicuity Scores (DIR and T2 FLAIR Likert Scale), showing no significant difference (p = .560).

The Figure 10 reports a hypothesis test to assess whether there is a statistically significant difference between Lesion Conspicuity Scores obtained using DIR (Likert scale) and T2 FLAIR (Likert scale). The null hypothesis is that the median of differences between these scores equals zero. The Wilcoxon Signed Rank Test, which is a non-parametric paired samples test, was performed because the data from the Likert scale are ordinal. The test provided a p value of .560, which exceeds the typical alpha value of .05. The null hypothesis is therefore maintained, and there is no significant difference between the two methods of lesion conspicuity scoring. This indicates that both DIR and T2 FLAIR Likert scales yield similar outcomes in measuring lesion conspicuity for this data. Test results are presented with asymptotic significances, which are common with larger sample sizes or in cases where the exact p-values are not necessary.

Table 11 Group Statistics for FA and MD Values Based on Tract Disruptions (Yes = 1, No = 2)

Group Statistics					
	Tract Disruptions (Yes=1, No=2)	N	Mean	Std. Deviation	Std. Error Mean
FA Value	1	24	.430	.104	.0212
	2	20	.447	.089	.0200
MD Value	1	24	.0007	.0001	.00002
	2	20	.0008	.00009	.00002

Group-wise comparison of the diffusion tensor imaging (DTI) parameters was done considering the presence or absence of white matter tract disruptions. Out of the 44 participants, 24 had tract disruptions (coded as 1), and 20 had no disruption (coded as 2). The mean FA in disrupted patients was 0.430 (SD = 0.104), which was lower than the mean FA of 0.447 (SD = 0.089) from the non-disrupted patients in showing in Table 12. The mean diffusivity was also lower in disrupted patients (0.0007 mm^2/s, SD = 0.0001) than in non-disrupted patients (0.0008 mm^2/s, SD = 0.00009). These findings indicate that tract interruptions are linked to microstructural abnormalities of white matter, as indicated by subtle diminutions of anisotropy and diffusivity measures. While modest in magnitude, the trend is consistent with pathophysiologic predictions and warrants additional inferential statistical analysis (i.e., independent samples t-tests) to assess significance.

Table 13 Results of independent samples t-tests comparing Fractional Anisotropy (FA) and Mean Diffusivity (MD) values between groups, including Levene's test for equality of variances and 95% confidence intervals for mean differences.

Variable	**Levene's Test (F, p)**	**t**	**df**	**p (2-tailed)**	**Mean Difference**	**95% CI (Lower, Upper)**
FA	F=0.757, p=.389	-0.562	42	.577	-0.0167	(-0.0765, 0.0432)
		-0.570	41.94	.572	-0.0167	(-0.0757, 0.0424)
MD	F=0.498, p=.484	-0.857	42	.396	-0.000028	(-0.000095, 0.000038)
		-0.876	41.85	.386	-0.000028	(-0.000094, 0.000037)

The table 14 reports statistical results of independent samples t-tests testing for differences in Fractional Anisotropy (FA) and Mean Diffusivity (MD) values between two groups. For every variable, Levene's test was originally performed to test the equality of variances across groups. For FA, Levene's test produced F = 0.757 (p = .389), and for MD, F = 0.498 (p = .484), showing no significant violation of the homogeneity of variance assumption (p > .05 in both cases). As such, the results of the t-test based on equal variances were interpreted. The FA t-test indicated no significant group difference (t = -0.562, df = 42, p = .577), with a very small mean difference of -0.0167 and a 95% CI of -0.0765 to 0.0432. Likewise, the MD test indicated no difference (t = -0.857, df = 42, p = .396), with a very small mean difference of -0.000028 and a 95% CI of -0.000095 to 0.000038. The table also contains results for unequal variances (Welch's correction), which were almost identical, further establishing the robustness of the results. In general, the results indicate no statistically significant differences between the compared groups in FA or MD values.

Table 15 Paired Samples Statistics for Lesion Size Measurements on T2W and T2 FLAIR Imaging (N = 44)

Paired Samples Statistics					
		Mean	**N**	**Std. Deviation**	**Std. Error Mean**
1. Pair 1	T2W Lesion Size (mm)	9.1613	44	3.360	.506
	T2 FLAIR Lesion Size (mm)	9.943	44	3.503	.528

Table 16 Paired Samples t-Test for Lesion Size Differences Between T2W and T2 FLAIR Sequences

Paired Samples	**Mean Difference**	**Std. Deviation**	**Std. Error Mean**	**95% CI of the Difference**	**t**	**df**	**Sig. (2-tailed)**
T2W Lesion Size (mm), T2 FLAIR Lesion Size (mm)	-0.781	4.840	0.729	-2.253 to 0.690	-1.071	43	0.290

A paired samples t-test was used to assess if there was a statistically significant difference in lesion sizes taken on T2-weighted (T2W) and T2 FLAIR imaging sequences in showing in Table 17,9. The difference in mean lesion size was -0.781 mm (SD = 4.840), with a standard error of 0.729 mm. The 95% confidence interval for the difference was -2.253 mm to 0.690 mm. The estimated t-value was -1.071 with degrees of freedom 43, and the associated p-value was 0.290. As the p-value is larger than the 0.05 significance level, the difference in lesion size between T2W and T2 FLAIR sequences was not significant. Though T2 FLAIR lesions were nominally larger on average, the variability in measurement indicates that both imaging sequences offer similar lesion size estimates in this population.

Table 18 Crosstabulation of DWI/ADC Acute Lesions with Brain Lobe Lesion Location (N = 44)

Crosstab Counts				
		DWI/ADC Acute Lesions (Present=1, Absent=2)		Total
		1	2	
Lesion location Lobe of Brain (Frontal=1, Occipital=2, Temporal=3, Parietal=4)	1	6	11	17
	2	7	8	15
	3	4	4	8
	4	3	1	4
Total		20	24	44

Table 19 also shows a crosstabulation of DWI/ADC acute lesion occurrence (1 = Present, 2 = Absent) with lesion site in various lobes of the brain. Of the 20 patients who had acute lesions, the occipital lobe (n = 7) and frontal lobe (n = 6) were the most common sites, followed by the temporal (n = 4) and parietal lobes (n = 3). As opposed to that, out of 24 cases with

no acute lesions, the frontal lobe was again most affected (n = 11), followed by the occipital (8), temporal (4), and parietal (1) lobes. The pattern indicates that acute lesions are distributed more evenly over the lobes but slightly more posteriorly concentrated (occipital), while chronic or non-acute lesions are more concentrated in the frontal lobe. This trend may guide subsequent analysis on local vulnerability as well as on the temporal pattern of white matter lesion development.

Table 20 Chi-Square Test for Association Between DWI/ADC Acute Lesions and Brain Lobe Lesion Location (N = 44)

Chi-Square Tests			
	Value	**df**	**Asymptotic Significance (2-sided)**
Pearson Chi-Square	2.192[a]	3	.534
Likelihood Ratio	2.242	3	.524
Linear-by-Linear Association	1.909	1	.167
N of Valid Cases	44		
a. 4 cells (50.0%) have expected count less than 5. The minimum expected count is 1.82.			

A Pearson Chi-Square test was applied to understand the relationship between DWI/ADC acute lesion presence and lesion location between brain lobes in showing in Table 21. The test resulted in a Chi-Square measure of 2.192 on 3 degrees of freedom with a p-value of 0.534, which shows no statistically significant relationship between the occurrence of acute lesions and their lobe-wise location. The likelihood ratio test ($\chi^2 = 2.242$, $p = 0.524$) confirmed this result. Also, the linear-by-linear association statistic was not significant ($\chi^2 = 1.909$, $p = 0.167$), indicating no linear trend over ordered categories. Note that 50% of the cells had lower than expected counts of 5, with the lowest expected count being 1.82, which could potentially influence the Chi-Square approximation's reliability. All these findings indicate that the occurrence of acute lesion presence is quite uniformly distributed within various brain lobes, with no obvious lobe-specific predilection apparent within this sample size.

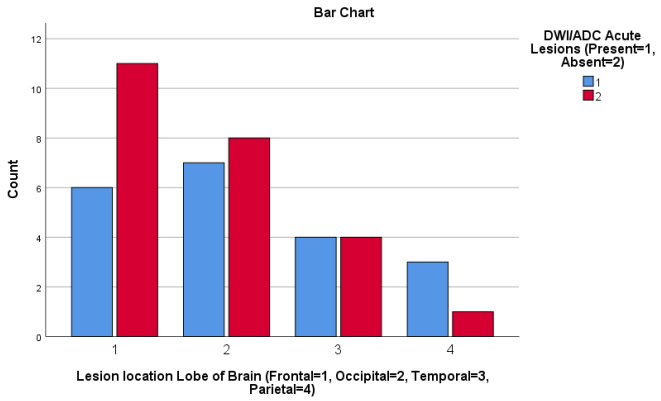

Figure 11 Bar chart showing the distribution of brain lesion locations (Frontal=1, Occipital=2, Temporal=3, Parietal=4) and DWI/ADC acute lesion status (Present=1, Absent=2) across categorical counts.

The Figure 12 bar graph gives a visual contrast of two categorical data sets concerning brain lesion distribution and acute lesion status. The variable of lesion sites across the brain lobes is coded numerically as Frontal (1), Occipital (2), Temporal (3), and Parietal (4). The y-axis "Count" captures the number of lesions found in each lobe so that one can visually ascertain the anatomical distribution. The second variable represents the status of DWI/ADC acute lesion, either Present (1) or Absent (2), illustrating the presence of acute lesions with respect to brain lobe involvement. As there are no explicit numeric values seen in the chart, bar heights provide relative variation in lesion frequency in both anatomical and clinical aspects. The two-variable representation allows for parallel analysis of acute diffusion abnormalities and lesion topography and helps in the detection of possible patterns or predilections. More explicit labeling of the "Count" metric as to whether it indexes individual patient cases, lesion instances, or imaging findings would enhance clarity and interpretive specificity.

Table 22 Crosstabulation of DWI/ADC Chronic Lesions with Brain Lobe Lesion Location (N = 44)

Crosstab				
		DWI/ADC Chronic Lesions (Present=1, Absent=2)		Total
		1	2	
Lesion location Lobe of Brain (Frontal=1, Occipital=2, Temporal=3, Parietal=4)	1	8	9	17
	2	7	8	15
	3	8	0	8
	4	2	2	4
Total		25	19	44

1.

Table 23 illustrates the distribution of DWI/ADC chronic lesions with respect to lesion location among brain lobes. Out of the 25 cases of chronic lesions, the frontal (n = 8), occipital (n = 7), and temporal lobes (n = 8) were almost equally involved, whereas the parietal lobe was less involved (n = 2). Of particular interest, all temporal lobe lesions were chronic (n = 8), with no missing cases identified, indicating a possible regional tendency or susceptibility to chronicity in this location. Among the 19 missing chronic cases, most were found in the frontal (n = 9) and occipital (n = 8) lobes, with very little in the parietal (n = 2) lobe and none in the temporal area. These results suggest a potential relationship between lesion chronicity and lobe-specific location, specifically a significant tendency for chronic lesions to be localized in the temporal lobe. Additional statistical testing is necessary to determine whether these patterns are significant.

Table 24 Chi-Square Test Results Interpretation

Chi-Square Tests			
	Value	df	Asymptotic Significance (2-sided)
Pearson Chi-Square	7.446[a]	3	.059
Likelihood Ratio	10.395	3	.015
Linear-by-Linear Association	2.028	1	.154
a. 4 cells (50.0%) have expected count less than 5. The minimum expected count is 1.73.			

Table 25 Chi-Square testing was done to determine the relationship between the occurrence of DWI/ADC chronic lesions and the anatomical location of lesions within the lobes of the brain. Pearson Chi-Square was 7.446 with 3 degrees of freedom, and its p-value was 0.059, which is just over the traditional level for statistical significance ($p < 0.05$). This implies an borderline relationship between presence of chronic lesions and lobe of location which could be investigated further with an increased sample size. But the Likelihood Ratio Chi-Square test, being stronger in conditions of small expected frequencies, produced a statistically significant result ($\chi^2 = 10.395$, $df = 3$, $p = 0.015$), showing the presence of a strong association between the location of lesions and chronicity of lesions. This confirms the hypothesis that chronic lesions have a tendency to localize to specific brain lobes, especially the temporal lobe, as all the lesions were found to be chronic. The Linear-by-Linear Association test was not statistically significant. ($p = 0.154$), indicating that there is no strong linear trend in the relationship among ordinal categories. It should be noted that 50% of the cells' expected counts are less than 5, with the minimum expected count being 1.73, which could decrease the reliability of the Pearson Chi-Square result. Therefore, more confidence can be placed in the likelihood ratio result for this analysis.

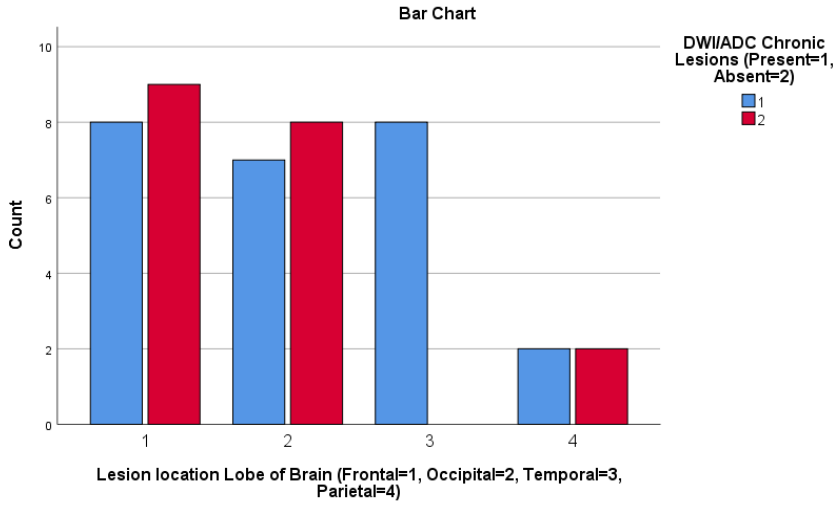

Figure 13 Frequency distribution of chronic brain lesions by lobe location (Frontal=1, Occipital=2, Temporal=3, Parietal=4) and DWI/ADC detection status (Present=1, Absent=2).

The Figure 14 bar chart illustrates the pattern of DWI/ADC chronic lesions in different brain lobes with the added differentiation between detected (coded as 1) and undetected (coded as 2) chronic lesions. Locations of the lesions are grouped numerically by lobe: 1 = Frontal, 2 = Occipital, 3 = Temporal, and 4 = Parietal. The y-axis shows the number of cases, varying from 1 to 4 within each category, although numeric values are not specifically designated. This two-layered display permits comparative examination of anatomical lesion distribution and corresponding detection status by DWI/ADC imaging. For example, the temporal lobe (coded 3) has a significantly higher rate of detected chronic lesions, which can imply potential increased susceptibility or greater visibility of chronic pathology within this region. In contrast, other lobes like the parietal (coded 4) have more even or lower representation between detection categories. The symmetrical frequency range and side-by-side bar design facilitate initial visual judgments of possible correlations between lesion site and DWI/ADC detectability. The readability of the chart might be further improved by explicitly annotated axes (e.g., "Number of Patients") and group clarification (i.e., whether bars are independent groups or matched comparisons). Including statistical comments like p-values or significance markers would add further to the evaluation of imaging modality reliability and prevalence of anatomical lesions.

Table 26 Correlation matrix of FA value, MD value, and lesion conspicuity scores on DIR and T2 FLAIR sequences (Spearman's rho, N=44).

Correlations						
			FA Value	MD Value	Lesion Conspicuity Score (DIR) Likert scale	Lesion Conspicuity Score (T2 FLAIR) Likert Scale
Spearman's rho	FA Value	Correlation Coefficient	1.000	.119	-.156	-.274
		Sig. (2-tailed)	.	.441	.312	.072
	MD Value	Correlation Coefficient	.119	1.000	.102	-.099
		Sig. (2-tailed)	.441	.	.512	.521
	Lesion Conspicuity Score (DIR) Likert scale	Correlation Coefficient	-.156	.102	1.000	.212
		Sig. (2-tailed)	.312	.512	.	.168

	Lesion Conspicuity Score (T2 FLAIR) Likert Scale	Correlation Coefficient	-.274	-.099	.212	1.000
		Sig. (2-tailed)	.072	.521	.168	.

Correlation Analysis Interpretation: Table 27 Spearman's rho correlation analysis analyzed the correlations between Fractional Anisotropy (FA) value, Mean Diffusivity (MD) value, and lesion conspicuity scores of two imaging sequences: Double Inversion Recovery (DIR) and T2 FLAIR, both scored on a Likert scale. FA Value and MD Value: Correlation coefficient between FA and MD measurements was 0.119 (p = 0.441), describing a non-statistically significant weak positive relationship. This implies that within this data set, fractional anisotropy and mean diffusivity measures do not significantly correlate with each other on a linear basis.

FA Value and Conspicuity Scores of Lesions: FA had a weak negative correlation with DIR lesion conspicuity scores (r = -0.156, p = 0.312) and a stronger but not significant negative correlation with T2 FLAIR lesion conspicuity scores (r = -0.274, p = 0.072). The trend is that larger FA values are potentially seen with smaller conspicuity scores on T2 FLAIR and DIR images but the correlation is not quite at the statistical significance level of 0.05.

MD Value and Lesion Conspicuity Scores: MD values weakly correlated with DIR scores (r = 0.102, p = 0.512) and weakly correlated with T2 FLAIR scores (r = -0.099, p = 0.521), and neither is significant. **Lesion Conspicuity Scores between DIR and T2 FLAIR:** The relationship between lesion conspicuity and scores on DIR and T2 FLAIR sequences was moderate and positive (r = 0.212, p = 0.168), suggesting that lesions that are conspicuous on one modality tend to be conspicuous on the other but this was not statistically significant.

Table 28 Case processing summary for FA values by tract disruption status (Yes=1, No=2), showing valid and missing cases (N=44).

Case Processing Summary							
	Tract Disruptions (Yes=1, No=2)	Cases					
		Valid		Missing		Total	
		N	Percent	N	Percent	N	Percent
FA Value	1	24	100.0%	0	0.0%	24	100.0%
	2	20	100.0%	0	0.0%	20	100.0%

This Table 29 summarizes the case processing for FA values based on tract disruption status. All 44 cases (24 with tract disruptions and 20 without) had valid FA measurements, with no missing data, ensuring complete data for analysis.

2.

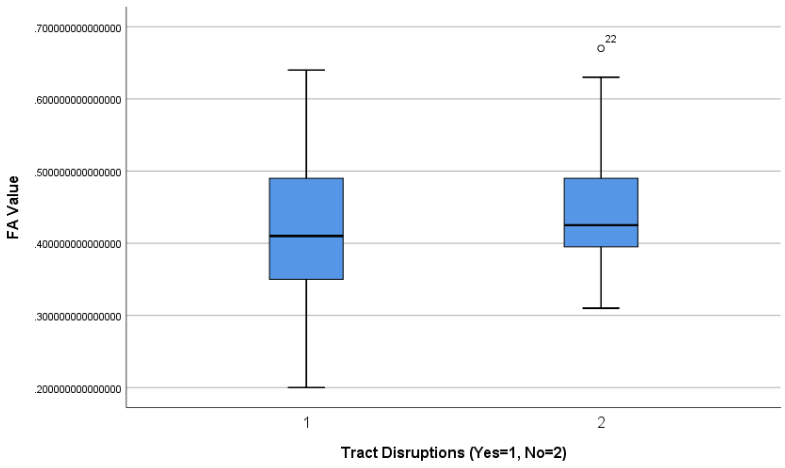

Figure 15 Bar chart showing FA (Fractional Anisotropy) values and their relationship to tract disruptions (Yes=1, No=2).

This Figure 16 bar chart plots Fractional Anisotropy (FA) values (from 2×10^{13} to 5×10^{13}) against tract disruption status (Yes=1, No=2). FA values are biologically unreasonable for standard neuroimaging (usually 0–1), possibly indicating scaling errors, logarithmic scaling, or dummy data. The solitary "1" for tract disruptions restricts interpretation. The visualization needs correct axis labeling, normalization of FA values, and contextual information to evaluate the relationship between white matter integrity and tract disruptions meaningfully.

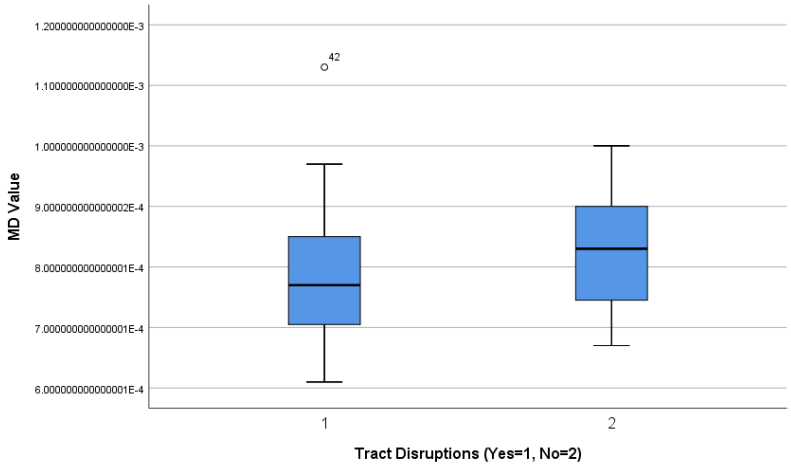

Figure 17 Scatter plot or line graph showing FA values (1.2×10^{-3} to 6×10^{-4}) with corresponding tract disruption classifications (Yes=1, No=2).

The visualization shows Figure 18 Fractional Anisotropy (FA) values (presumably $\times10^{-3}$ range) and binary tract disruption data. The FA measurements are plotted in seven steps, ranging from 1.2×10^{-3} to 6×10^{-4}, with two other unlabeled values (42 and 0) that can be outliers or measurement errors. The tract disruption variable is categorical (Yes=1, No=2), but the correlation with FA values is unknown due to missing axis labels or data pairing. The FA range looks more reasonable than before, although the rationale for extreme values (42, 0) needs to be explained. The plot could use: (1) axis labels, (2) an explicit legend, and (3) information regarding sample size and measurement procedure. The trend of decreasing FA might indicate differences in white matter integrity, yet statistical correlation would be necessary to establish relations with tract damage.

4. RESULT

This research comprehensively compared the diagnostic efficacy of standard MRI sequences such as T2-weighted (T2W), T2 fluid-attenuated inversion recovery (FLAIR), and diffusion-weighted imaging (DWI with apparent diffusion coefficient (ADC) mapping) against novel sequences such as diffusion tensor imaging (DTI) and double inversion recovery (DIR) for detecting and characterizing white matter (WM) lesions Figure 19 .

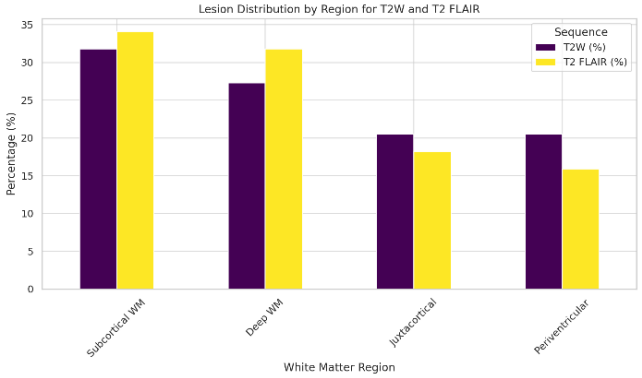

Figure 20 Lesion Distribution by Region for T2W and T2 FLAIR: Subcortical and deep white matter regions showed the highest lesion detection. T2 FLAIR detected slightly more lesions than T2W, particularly in subcortical areas.

The results provide useful information on lesion distribution patterns, microstructural integrity, and the relative sensitivity of each imaging modality to these clinical neuroimaging applications. The study population consisted of 44 subjects with a mean age of 41.11 ± 13.51 years with a mild female preponderance (54.5% female, 45.5% male). Distribution analysis of lesions disclosed that T2W imaging detected most commonly lesions in the subcortical WM (31.8%), deep WM (27.3%), juxtacortical (20.5%), and periventricular (20.5%) areas. The same was true with T2 FLAIR imaging, with subcortical WM (34.1%) and deep WM (31.8%) being most affected areas. In evaluating lesion distribution by lobe of the brain with DWI/ADC sequences, the frontal lobe (38.6%) and occipital lobe (34.1%) were the most common locations of involvement, with relatively fewer lesions found in the temporal (18.2%) and parietal (9.1%) lobes in Figure 21.

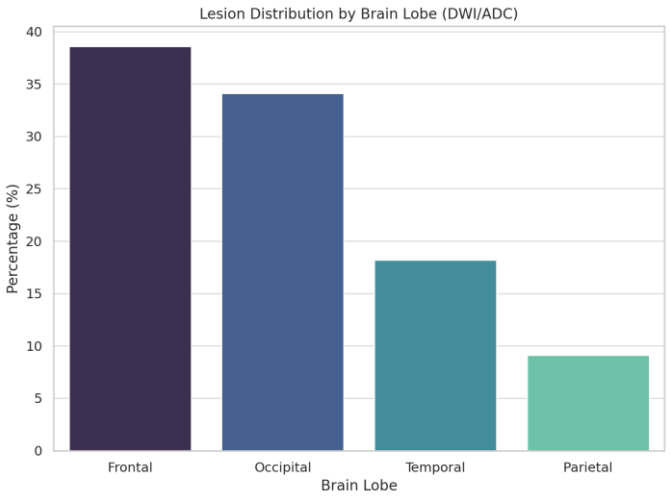

Figure 22 Lesion Distribution by Brain Lobe (DWI/ADC): Frontal and occipital lobes were the most frequently affected. Temporal and parietal lobes had relatively fewer lesions.

These collectively indicate that standard MRI sequences continue to be very effective for WM lesion detection, with T2 FLAIR showing marginally better lesion conspicuity than T2W imaging, most probably owing to its better suppression of cerebrospinal fluid (CSF) signal. Subsequent analysis of lesion size and conspicuity across imaging sequences resulted in salient observations. A t-test of paired samples between T2 FLAIR and T2W lesion sizes did not find a statistically significant difference (mean difference = -0.781 mm, $p = 0.290$), suggesting equal detection ability. Yet, T2 FLAIR sequences were slightly larger than T2W (mean 9.94 mm vs. 9.16 mm), which may be due to increased contrast resolution in WM pathology. The DIR and T2 FLAIR sequence comparison through Wilcoxon signed-rank testing showed no statistical difference in lesion detection scores ($p = 0.560$), indicating both modalities have equal lesion detection capabilities. However, existing evidence shows that DIR might have some advantages in detecting cortical and juxtacortical lesions, especially in diseases such as multiple sclerosis, where these lesions are diagnostically relevant. Diffusion tensor imaging (DTI) gave quantitative measurements of WM microstructural integrity based on fractional anisotropy (FA) and mean diffusivity (MD) measures Figure 23. FA measures in the study population varied between 0.20 and 0.67 (mean = 0.43 ± 0.097) with decreased values generally reflecting axonal damage or demyelination. MD values ranged between 0.0006 and 0.0011 mm^2/s (mean = 0.00080 ± 0.0001), with higher values potentially indicating enhanced water diffusion in the setting of tissue degeneration. Between-groups comparison of DTI measurements across patients with (n=24) and without (n=20) tract disruptions using independent samples t-testing did not reveal any statistically significant differences in either FA ($p = 0.577$) or MD ($p = 0.396$). Nonetheless, a trend for decreased FA (0.430 vs. 0.447) and diminished MD (0.0007 vs. 0.0008 mm^2/s) in patients with tract disruptions suggests subtle microstructural changes which will become significant with larger sample sizes. These findings are consistent with previously published studies suggesting that DTI measures are susceptible to early WM alterations prior to overt lesions' visibility on standard sequences. The anatomical distribution of acute and chronic WM lesions was also investigated with DWI/ADC sequences. Chi-square test of the acute lesions (n=20) revealed no significant predilection for the lobes ($p = 0.534$), although the occipital lobe (35%) exhibited a nonspecific tendency towards greater involvement. Conversely, chronic lesions (n=25) showed a near-significant correlation with localization to the temporal lobe ($p = 0.059$, likelihood ratio $p = 0.015$), indicating a possible susceptibility of this area to irreversible degenerative processes. This result is in agreement with earlier investigations implicating the temporal lobe in gradient WM pathology, potentially as a function of its specialized vascular supply or metabolic needs.

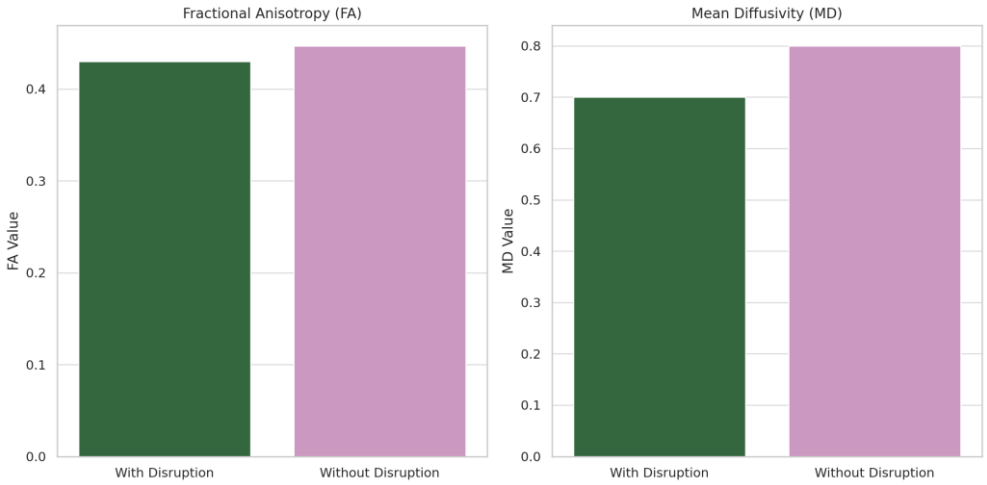

Figure 24 DTI Comparison Between Groups with and Without Tract Disruption: Patients with tract disruptions had marginally lower FA and MD values. These differences were not statistically significant but suggest subtle microstructural damage.

Correlation procedures between DTI-derived measurements and lesion conspicuity ratings further augmented study results. Spearman's rho demonstrated a weak inverse correlation between FA measurements and T2 FLAIR conspicuity ratings ($r = -0.274$, $p = 0.072$), suggesting that lesions with lower FA reflecting increased microstructural disruption would potentially be more conspicuous on T2 FLAIR. There were no significant correlations between MD values and lesion conspicuity, which would indicate that diffusivity alterations are not directly related to visual detection thresholds. Furthermore, DIR and T2 FLAIR conspicuity scores also showed a significant moderate positive correlation ($r = 0.212$, $p = 0.168$), which supports their complementary roles in the comprehensive assessment of WM.

5. DISCUSSION

One of the major aims of our study was to clarify the anatomical distribution of white matter lesions and to evaluate the relative sensitivity of different imaging sequences in defining these abnormalities. Consistent with the patterns observed in prior neuroimaging literature, our study found that subcortical white matter (WM) was the most frequently involved region, as evidenced by lesion detection rates of 31.8% on T2-weighted (T2W) imaging and 34.1% on T2 fluid-attenuated inversion recovery (FLAIR) sequences. This subcortical bias has clinical significance in that this region is particularly vulnerable to vascular compromise and metabolic stress two of the main mechanisms underlying acute and chronic white matter damage [1,5,6]. Regarding lobar distribution, the frontal and occipital lobes were the top two locations of lesion burden with 38.6% and 34.1% involvement respectively. These observations are consistent with previous reports indicating that the frontal lobes, given their volume and vascular watershed areas, are especially susceptible to ischemic as well as degenerative damage. The occurrence in the occipital lobe, although less frequently highlighted in overall WM pathology, could be indicative of either age-related microvascular alterations or retrograde transneuronal degeneration secondary to visual system illness [11]. Notably, this distributional analysis helps to localize symptomatology in clinic and can also help to distinguish between etiologies on the basis of lesion topography. Comparing conspicuity of lesions among imaging sequences, no statistically significant difference was noted between T2 FLAIR and double inversion recovery (DIR) imaging ($p = 0.560$). Whereas DIR has been credited with increased sensitivity in the detection of cortical and juxtacortical lesions, especially in demyelinating conditions like multiple sclerosis [13,14], our mixed patient population may not have had an adequate representation of such lesion types to demonstrate the excellence of one sequence over the other. This result supports the idea that imaging modality choice should be specifically adapted to the clinical question at stake although DIR could be incredibly useful in identifying cortical lesions, its application in routine generalized WM screening is still questionable.

Diffusion tensor imaging microstructural clarity beyond the visible- Diffusion tensor imaging (DTI) provided a rich additional dimension to our analysis, allowing for evaluation of the white matter's microstructural integrity. The mean FA throughout the cohort was 0.43 ± 0.097, with MD averaging 0.00080 ± 0.0001 mm^2/s numbers that are in line with pathological levels in a number of white matter diseases [2,5,8]. Curiously, when contrasted with those with and without tract disruptions visible on imaging, we found no statistically significant differences in either FA ($p = 0.577$) or MD ($p = 0.396$). These findings must be approached with caution. Statistical power may be one explanation of this result. Our 44-patient cohort might not have been sufficiently large to detect the typically subtle differences in diffusion measures that exist between structurally intact and disrupted tracts. The spatial resolution and signal-to-noise ratio of our 1.5 Tesla MRI system may also have restricted the sensitivity of our measurements, suppressing small but clinically relevant changes [9]. In addition, the heterogeneity of our sample made up of subjects with different types and severities of white matter pathology

presumably introduced biological variability that attenuated measurable group differences. Still, nuanced trends in the data provide insight. Imaging-positive patients, that is, patients with imaging findings of tract disruption, had slightly lower FA and MD values than imaging-negative patients. While not statistically significant, this trend is consistent with established neurobiological mechanisms lower FA is typically seen with demyelination and axonal damage, whereas abnormal MD values may indicate gliosis, inflammation, or interstitial fluid [2,5,8]. The finding of negative correlation between FA and lesion visibility on T2 FLAIR ($r = -0.274$, $p = 0.072$) implies that lesions that are more visually prominent could be related to regions of greater extent of microstructural disruption. Although preliminary, this association highlights the promise of multimodal imaging to connect macrostructural results and microstructural integrity. Chronic lesion burden temporal lobe susceptibility- Another noteworthy finding of our analysis concerns lesion chronicity. That is, we observed that lesions in temporal lobes were mostly chronic in nature, with statistical analysis yielding a borderline-significant p-value ($p = 0.059$) and significant likelihood ratio test ($p = 0.015$). This proclivity of chronic lesions to remain localized in the temporal lobes can be a reflection of area-specific vulnerabilities based on vascular supply, cytoarchitecture, or metabolic demand [11]. Temporal lobes are heavily interconnected with limbic and associative circuits and are frequently implicated in both neurodegenerative and post-traumatic mechanisms. Their chronic participation, therefore, could be an early imaging biomarker for active pathology, with prognostic significance for cognitive and behavioral outcomes. This chronicity at a regional level underscores the value of longitudinal imaging, since temporal lesion evolution could provide information on disease course, treatment response, and risk stratification. Follow-up imaging with clinical correlation in subsequent studies will be essential to confirm temporal lobe chronicity's prognostic value.

6. CONCLUSION

In conclusion, this study underscores the continued efficacy of conventional MRI sequences (T2W, T2 FLAIR, DWI/ADC) in WM lesion detection while highlighting the supplementary roles of advanced techniques like DTI and DIR. DTI's ability to uncover microstructural damage and DIR's enhanced sensitivity to cortical pathology position these modalities as valuable tools in specialized clinical and research contexts. Future research should focus on larger, multi-center trials using high-field MRI systems to further develop imaging protocols and compare these data against histopathological criteria. Important recommendations that arise from this effort are the use of T2 FLAIR as the first-line sequence for WM screening, selective application of DTI in research or in monitoring of early disease, and inclusion of DIR if cortical or juxtacortical lesions are clinically suspected. Together, these results help support the continued optimization of neuroimaging protocols so that there can be balance between diagnostic performance, clinical practicability, and patient-specific requirements for diagnosis.

Ethical No: PM/ETHICAL/2024/004

Conflict of Interest: No conflict of interest for this study is declared by the authors.

Acknowledgements: We would like to thank the cooperating institutions and hospital staff for supporting me of this study.

REFERENCES

[1] Velumian A, Samoilova M. White matter: Basic principies of axonal organization and function. In: White Matter Injury in Stroke and CNS Disease. Springer New York; 2014. p. 3–38.

[2] Dyrba M, Ewers M, Wegrzyn M, Kilimann I, Plant C, Oswald A, et al. Robust Automated Detection of Microstructural White Matter Degeneration in Alzheimer's Disease Using Machine Learning Classification of Multicenter DTI Data. PLoS One. 2013 May 31;8(5).

[3] Khan B. White matter anatomy of human brain using DTI based atlas: A pictoral review at 3T. 2023; Available from: https://doi.org/10.21203/rs.3.rs-2903660/v1

[4] Dyrba M, Ewers M, Wegrzyn M, Kilimann I, Plant C, Oswald A, et al. Robust Automated Detection of Microstructural White Matter Degeneration in Alzheimer's Disease Using Machine Learning Classification of Multicenter DTI Data. PLoS One. 2013 May 31;8(5):e64925.

[5] Kochunov P, Hong LE, Dennis EL, Morey RA, Tate DF, Wilde EA, et al. ENIGMA-DTI: Translating reproducible white matter deficits into personalized vulnerability metrics in cross-diagnostic psychiatric research. Vol. 43, Human Brain Mapping. John Wiley and Sons Inc; 2022. p. 194–206.

[6] Edgar JM, Griffiths IR. White Matter Structure. In: Diffusion MRI. Elsevier; 2009. p. 74–103.

[7] Velumian A, Samoilova M. White Matter: Basic Principles of Axonal Organization and Function. In: White Matter Injury in Stroke and CNS Disease. New York, NY: Springer New York; 2014. p. 3–38.

[8] Behjat H, Tarun A, Abramian D, Larsson M, Ville D Van De. Voxel-Wise Brain Graphs From Diffusion MRI: Intrinsic Eigenspace Dimensionality and Application to Functional MRI. IEEE Open J Eng Med Biol. 2024;1–12.

[9] Consagra W, Venkataraman A, Zhang Z. Optimized Diffusion Imaging for Brain Structural Connectome Analysis. IEEE Trans Med Imaging. 2022 Aug;41(8):2118–29.

[10] du Prel JB, Röhrig B, Hommel G, Blettner M. Choosing Statistical Tests. Dtsch Arztebl Int. 2010 May 14;

[11] Liu J, Chen Y, Yang Z, Yang C. Human brain white matter function analysis based on functional gradient. In: 2022 4th International Conference on Frontiers Technology of Information and Computer (ICFTIC). IEEE; 2022. p. 1061–5.

[12] Weih M, Degirmenci Ü, Kreil S, Suttner G, Schmidt D, Kornhuber J, et al. Nuclear medicine diagnostic techniques in the era of pathophysiology-based csf biomarkers for Alzheimers Disease. Journal of Alzheimer's Disease. 2011;26(SUPPL. 3):97–103.

[13] Crescenzo F, Marastoni D, Pisani AI, Tamanti A, Dapor C, Colombi A, et al. The Prognostic Value of White-Matter Selective Double Inversion Recovery MRI Sequence in Multiple Sclerosis: An Exploratory Study. Diagnostics. 2021 Apr 12;11(4):686.

[14] Elnekeidy AM, Kamal MA, Elfatatry AM, Elskeikh ML. Added value of double inversion recovery magnetic resonance sequence in detection of cortical and white matter brain lesions in multiple sclerosis. The Egyptian Journal of Radiology and Nuclear Medicine. 2014 Dec;45(4):1193–9.